Desalination and Water Treatment
www.deswater.com

doi: 10.1080/19443994.2015.1060536

57 (2016) 13747–13759
June

Taylor & Francis
Taylor & Francis Group

Investigation of heavy metal ions adsorption by magnetically modified aloe vera leaves ash based on equilibrium, kinetic and thermodynamic studies

Somayeh Abedi, Hassan Zavvar Mousavi*, Alireza Asghari

Department of Chemistry, Semnan University, Semnan, Iran, Tel. +98 231 3366194; Fax: +98 231 3354110;
emails: sabedi48@yahoo.com (S. Abedi), hzmousavi@semnan.ac.ir (H. Zavvar Mousavi), aasghari@semnan.ac.ir (A. Asghari)

Received 15 December 2014; Accepted 3 June 2015

ABSTRACT

Magnetically modified aloe vera leaves ash (MALA) was prepared, characterized, and used for simultaneous removal of Pb(II), Cu(II), Zn(II), and Cr(III) ions from aqueous solutions. MALA was prepared by treating ALA with Fe_3O_4 nanoparticles. Effects of different parameters on the batch adsorption experiments were studied and optimized by both the magnetic and non-magnetic ALA. The kinetic and isotherm experimental data were well described by the pseudo-second-order kinetic model and the Langmuir isotherm model, respectively. Thermodynamic studies indicated that the adsorption processes were spontaneous and exothermic in nature. The adsorption process of MALA was fast and removal efficiencies were higher than 98% under the optimized conditions. MALA could be reused with suitable recovery after hydrochloric acid washing. It was indicated that the developed method based on MALA is very simple, low cost, fast, and reliable for removal of heavy metal ions from water samples.

Keywords: Removal; Heavy metals; Magnetic aloe vera leaves ash; Isotherm; Kinetic

1. Introduction

Rapid industrialization has contributed to the release of toxic heavy metals to water streams. Some of the main sources of heavy metal ions in the environment include electroplating, metallurgical, tannery, and chemical manufacturing; and mining, pesticide, fuel production, and battery manufacturing industries. Heavy metals have harmful effects on human physiology and biological systems, such as kidneys, brain cells, and liver, when the concentration of heavy metal ions in human body exceeds the tolerance levels. Unlike organic wastes, heavy metals are not biodegradable and tend to accumulate in living organisms, causing various diseases and disorders; therefore, they must be removed before discharge in environment [1,2].

A number of methods are available for removal of toxic heavy metal ions from aqueous solutions, including chemical precipitation, chemical oxidation/reduction [3], membrane technologies [3,4], reverses osmosis [5], ion exchange [6], ion flotation [7], and adsorption. Among these techniques, adsorption technology is regarded as the most promising one to remove heavy metal ions from effluents due to its clean and fast operation, high efficiency, ease of handling, low cost, and availability of different adsorbents. The economy of this method depends mainly on the cost of the adsorbent materials [3,8,9]. Many researchers around the world are trying to evaluate

---

*Corresponding author.

adsorption capacities of different materials to find out more efficient and low-cost adsorbents for removal of heavy metal ions from aqueous solutions. Materials locally available in large quantities, such as natural materials, agricultural waste, or industrial byproducts, can be utilized as low-cost adsorbents [10–13].

Reusing agricultural waste products is one goal of environmental sustainability and has become an option to add value to producers. Agricultural wastes are an abundant source for significant metal ion sorption which have many advantages for wastewater treatment, including free availability, simple technique, requires little processing, good adsorption capacity, selectivity, low cost, and easy regeneration [14]. A large quantity of agricultural wastes, such as rice straw [15], grape stalk wastes [16], maize cob [17], orange peels [18], rice husks [19], eucalyptus bark [20], various leaves [8,21–23], and sawdust [24,25], etc. have been used as low-cost adsorbents for removal of toxic heavy metal ions from aqueous solutions.

Recently, magnetic separation has been considered as an effective and quick method for solid–liquid phase separation after the adsorption. Over the last few years, great interest is devoted to the development of magnetically modified agricultural adsorbents (MMAA), which can be separated, recycled, and easily used, especially on an industrial scale [26,27]. The main advantages of this technology include less contamination of sorbent and high capacity of treating large amount of metal ions in wastewater within a short time [28]. Magnetite nanoparticles (Fe_3O_4) as the commonly used magnetic material are combined with plant adsorbents owing to their easy sample preparation and good biocompatibility. Their basic properties, such as extremely small size and high surface area-to-volume ratio, provide better kinetics for the adsorption of metal ions from aqueous solutions [27,28]. Furthermore, the MMAA can stabilize the iron oxide nanoparticles by surface modification, hence protect them against oxidation and prevent their aggregation in aqueous systems [28–30]. Although there are many studies related to the using of agricultural adsorbents, only a few studies have been focused on the removal of contaminants using MMAA. These include the using of magnetic nanoparticles-impregnated tea waste [31,32], gum Arabic-modified magnetic nanoparticles [33], magnetically modified spent coffee grounds [29], magnetically modified spent grain [34], magnetic fluid-modified peanut husks [35], and magnetic-activated carbons from agricultural wastes [27,36].

The main purpose of the present study is to develop a new magnetically modified agricultural adsorbent for simultaneous removal of Pb(II), Cu(II), Zn(II), and Cr(III) ions from aqueous solutions. This adsorbent is prepared by mixing of aloe vera leaves ash (ALA) as a low-cost adsorbent with magnetite (Fe_3O_4) nanoparticles. Aloe vera leaves are one of the pharmaceutical, cosmetic, and food industries wastes that recently have been used as a power potential adsorbent for removal of Cr(VI) in aqueous solutions [37,38].

Different experimental conditions, such as solution pH, adsorbent dose, contact time, and temperature, for the maximum removal of all metal ions by both the magnetic and non-magnetic ALA were investigated and optimized. Meanwhile, behaviors and mechanisms of heavy metal ions adsorption were comprehensively explored by kinetic and isotherm models as well as thermodynamic parameters.

2. Experimental

2.1. Chemical reagents and materials

Experiments were conducted with aloe vera leaves collected from Semnan, Iran. Iron(III) chloride hexahydrate, iron(II) chloride tetrahydrate, and ammonia solution were supplied by Sigma-Aldrich (M) Sdn. Bhd., Malaysia. Metal nitrates, sodium hydroxide, and all of the other reagents used for experiments and analysis were of analytical grade and purchased from Merck (Darmstadt, Germany). Deionized water (DI-water) obtained from a Millipore Continental Water System (Bedford, MA, USA) was used throughout this study. Stock solutions were prepared from an appropriate amount of the nitrate salts of Pb(II), Cu(II), Zn(II), and Cr(III) as 1,000 mg L^{-1} solutions in DI-water. Standard solutions were prepared daily by dilution of the stock solutions.

2.2. Preparation of ALA

The aloe vera leaf was cut off from the plant and its latex was drained. The leaves were then washed with DI-water, and dried in a convection oven at 110˚C for 15 h. The ALA was prepared by burning the dried leaves at 500˚C in a muffle furnace for 5 h.

2.3. Synthesis of Fe_3O_4 nanoparticles

The simplest and efficient method based on co-precipitation was used for synthesis of the magnetite nanoparticles [39]. At first, 2.35 g of $FeCl_2{\cdot}4H_2O$ and 6.1 g of $FeCl_3{\cdot}6H_2O$ were dissolved under inert atmosphere in 100 mL of DI-water with vigorous stirring. Then, 30 mL of ammonium hydroxide solution (25%) was added dropwise to the solution with stirring at 80˚C. The reaction was allowed for 30 min at 80˚C under constant stirring to ensure the complete growth of nanoparticle crystals. During the reaction process, the pH was maintained at about 10. The resulting suspension was cooled down to room temperature and then Fe_3O_4 precipitant was separated with a magnet, washed several times with DI-water and finally dried in an oven at 50°C. The reaction that occurs in the preparation of magnetic nanoparticles is as follows:

$$2FeCl_3.6H_2O + FeCl_2.4H_2O + 8NH_4OH \rightarrow Fe_3O_4 + 8NH_4Cl + 20H_2O \quad (1)$$

2.4. Preparation of magnetically modified ALA (MALA)

The as-prepared ALA was first activated with HNO_3 solution. For this, ALA was washed by HCl solution (0.001 mol L^{-1}) to remove all salts precipitated in its pores, and then several times with DI-water to remove all traces of the acid. Subsequently, it was oven-dried at 80°C for 24 h to volatilize the organic impurities. Then, ALA was added to HNO_3 solution (0.001 mol L^{-1}) and remained at room temperature for 3 h. The mixture was then oven-dried at 60°C. Finally, 1 g of Fe_3O_4 nanoparticles was added into 10 mL of the aqueous suspension of activated ALA (100 mg mL^{-1}) in a 25 mL glass stoppered bottle. The reaction mixture was mixed at room temperature for 1 h (120 rpm) and then oven-dried at 80°C for 3 h.

2.5. Apparatus and characterization methods

Heavy metals analysis was carried out using atomic absorption spectrophotometer (Shimadzu, AA-680/G, Japan) under the conditions given by the manufacturer with air-acetylene flame. The pH values were measured with a Metrohm pH-meter (E-632, Herisau, Switzerland) supplied with a glass-combined electrode. A temperature-controlled orbital shaker (Technal, TE 4200, Brazil) was used in batch adsorption experiments. The morphology of the sorbent was studied using scanning electron microscopy (SEM, Phillips, PW3710, Netherland) and transmission electron microscopy (TEM, CM30, Philips, Netherland). SEM images of the adsorbents were obtained using scanning electron microscopy (SEM, Phillips, AIS2200, Korea). The morphology of the magnetic nanoadsorbent was examined by transmission electron microscopy (TEM, CM30, Philips, Netherland).

2.6. Adsorption procedure

Adsorption experiments were performed using batch technique to identify the effect of important variables, such as solution pH, adsorbent dosage, contact time, and temperature, on the adsorption of metal ions from aqueous solution.

Batch adsorption experiments were carried out in a series of 250 mL Erlenmeyer flasks containing 100 mL aqueous solutions of Pb(II), Cu(II), Zn(II), and Cr(III) ions with the initial concentration of 100 mg L^{-1} (from each one). Desired pH values were adjusted with 0.1 mol L^{-1} HCl or 0.1 mol L^{-1} NaOH. Appropriate amount of the sorbent was then added to each solution. The flasks were shaken in orbital shaker with 170 rpm speed at a constant temperature. Samples were withdrawn at regular time intervals and MALA was magnetically separated from the solutions (filtration through a Whatman filter paper in the case of ALA). The residual concentrations of metal ions in the sample solutions were determined using flame atomic absorption spectrophotometer. The adsorption tests were continued until the equilibrium concentration was reached. The removal percentage was calculated as:

$$\text{Removal}\,(\%) = \frac{(C_0 - C_e)}{C_0} \times 100 \quad (2)$$

The solid-phase heavy metal concentration, q_e (mg g^{-1}), was also determined using the following equation:

$$q_e = \frac{(C_0 - C_e)}{m} \times V \quad (3)$$

where C_0 and C_e are the initial and final concentrations (mg L^{-1}) of metal ions in solution phase, respectively; V is the volume of the treated solution (L); and m is the mass of adsorbent (g). All the experimental data were the averages of triplicate determinations.

2.7. Adsorption isotherm

In order to determine the adsorption isotherm model, equilibrium adsorption experiments were done in a batch mode. For this, 0.005 g of MALA and 100 mL of aqueous metal ions solution with various concentrations of 25, 35, 45, 55, 65, 75, 85, and 100 mg L^{-1} (pH 6) were shaken in 250 mL Erlenmeyer flasks at 170 rpm and 25°C for 10 min. The adsorbent dosage and contact time were 0.01 g and 7 min in the case of ALA. The equilibrium amount of metal ion adsorbed per unit mass of adsorbent was calculated using Eq. (3).

2.8. Adsorption kinetics

Adsorption kinetic model of the present study was investigated in batch mode. A series of 250 mL Erlenmeyer flasks containing the adsorbent and

100 mL of 100 mg L^{-1} metal ions solution were prepared. The pH, adsorbent dosage, and temperature were adjusted at 6, 0.005 g MALA (or 0.01 g ALA), and 25˚C, respectively. The flasks were shaken with 170 rpm speed at different contact times (1–20 min). The amount of metal ion adsorbed per unit mass of adsorbent at any time was calculated using Eq. (3).

2.9. Adsorption thermodynamics

A series of 250 mL Erlenmeyer flasks containing 0.005 g of MALA and 100 mL of 35 mg L^{-1} aqueous solution of metal ions at pH 6 were shaken with 170 rpm speed at different temperatures (15–65˚C) for 10 min. The adsorbent dosage, metal ions concentrations, and contact time were 0.01 g, 65 mg L^{-1}, and 7 min, respectively. The equilibrium amount of metal ion adsorbed per unit mass of adsorbent was calculated using Eq. (3).

3. Results and discussion

3.1. Characterization of adsorbent

In the present study, magnetically modified aloe vera leaves ash (MALA) was prepared by the combination of ALA with magnetite nanoparticles through the hydroxyl groups of the activated ALA. Scanning electronic microscope (SEM) is a widely used technique to study the morphological features of the adsorbents. SEM images of ALA, MALA, before and after metal ions adsorption with MALA are shown in Fig. 1((a)–(c)). An observation of the SEM micrograph of ALA (Fig. 1(a)) indicated the presence of many pores and a rough structure on the surface of this adsorbent, which was favorable for adsorption of heavy metal ions. Moreover, the active sites were available at 5 micro meters. As shown in Fig. 1(b), the Fe_3O_4 nanoparticles were completely incorporated into the ALA, and all the iron oxide particles were aggregated to form a spherical and cage-like structure. Furthermore, the active sites could be observed at 500 nm since the magnetite particles were occupying the active sites. Fig. 1(c) shows the SEM image after the adsorption of heavy metal ions onto MALA. Compared to Fig. 1(b), a significant change was observed at the surface of MALA, which was an evidence of the metal ions adsorption.

TEM image of MALA is shown in Fig. 2. Obviously, the spherical magnetite nanoparticles with smooth surface exhibited slight aggregation as a result of combination with ALA, which led to the formation of a magnetite core-ALA shell structure.

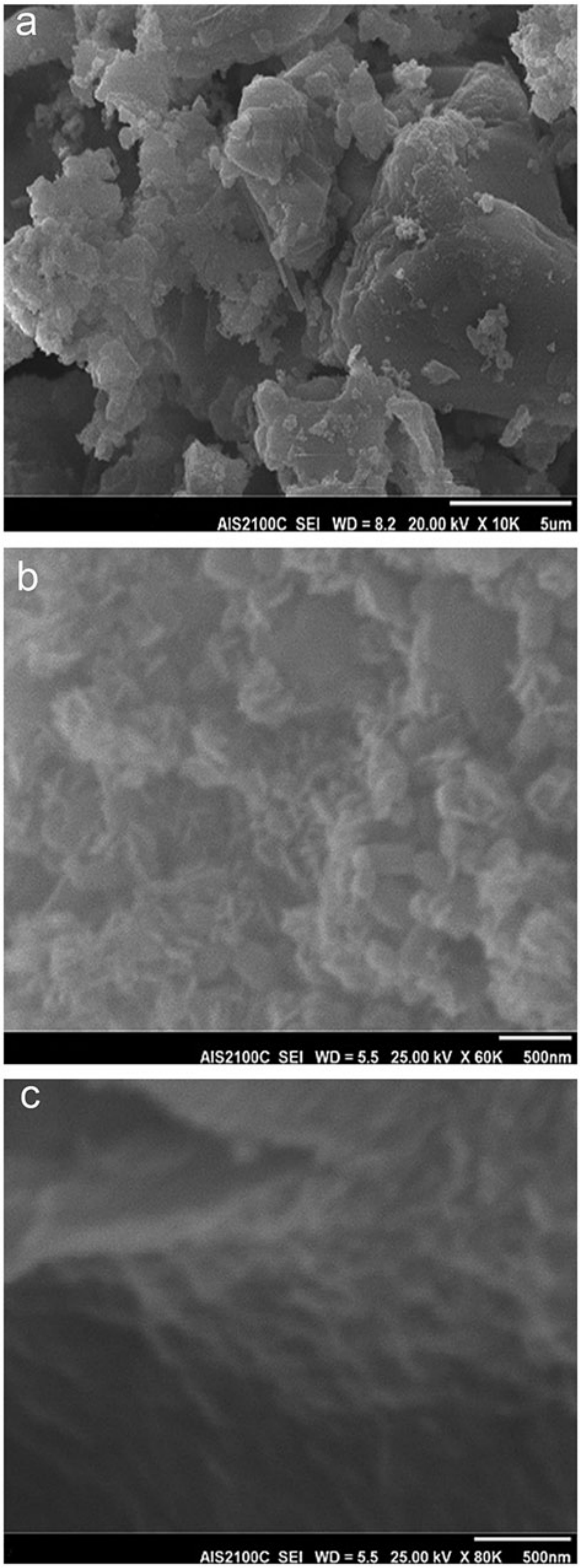

Fig. 1. SEM images of (a) ALA, (b) MALA, (c) M (II)-MALA.

3.2. Effect of pH

The pH of the solution has a significant impact on the uptake of heavy metal ions since it determines the surface charge of the adsorbent, the degree of ionization, and speciation of the adsorbate [40]. The effect of pH on the adsorption of heavy metal ions with 0.05 g MALA and 0.12 g ALA was studied separately over the pH range of 2–7 (to avoid metal ions precipitation), with known concentration of metal ions (100 mg L^{-1}) and contact time of 10 min at 25℃. As illustrated in Fig. 3, removal percentage of the metal ions increased from pH 2 to 7. The maximum removal of heavy metal ions was found to occur at pH 6–7. Accordingly, pH 6 was chosen as the optimal pH for all further studies. Similar results have also been reported by other investigators [41,42].

The most abundant surface functional group participating in the reactions on oxide surfaces is the hydroxyl group, which is amphoteric and reactive. Depending on the solution pH, the oxide surface can undergo protonation (Eq. (4)) or deprotonation (Eq. (5)) reactions:

$$-\mathrm{ROH} + \mathrm{H}^{+} \leftrightarrow -\mathrm{ROH}_2^{+} \tag{4}$$

$$-\mathrm{ROH} \leftrightarrow -\mathrm{RO}^{-} + \mathrm{H}^{+} \tag{5}$$

where R and OH represent the surface of the adsorbent and oxygen-containing groups, respectively. So, according to the solution pH, the surface is charged differently and could behave as an anion or cation exchanger. Therefore, low removal percentage of metal ions at low pH range is due to the electrostatic repulsion between the metal ions and positively charged sorbent surface. However, as the pH increases, the surface charge of both the adsorbents is more negative because of the deprotonation mechanism (Eq. (5)) and the RO^{-} becomes the dominating species. So, the electrostatic attraction (Eq. (6)) between negatively charged adsorbent surface and positively charged metal ions increases, which plays an important role in the adsorption process.

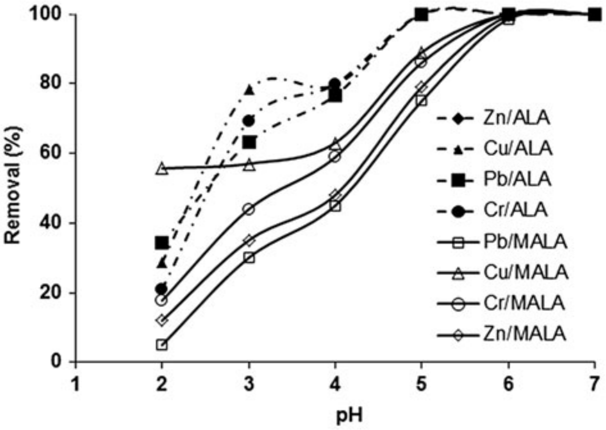

Fig. 3. Effect of initial pH on the adsorption of metal ions onto MALA and ALA (100 mL of 100 mg L^{-1} metal ions solution; mALA = 0.12 g, mMALA = 0.05 g; t = 10 min; T = 25℃).

$$n\,\mathrm{R}-\mathrm{O}^{-} + \mathrm{M}^{2+} \rightarrow (\mathrm{R}-\mathrm{O}^{-})_n\mathrm{M}^{(2-n)+} \tag{6}$$

where $(R\text{-}O^{-})_n\ M^{(2-n)+}$ corresponds to the surface complexes and n is the stoichiometric coefficient. Similar mechanism has also been reported in the study carried out by Banerjee and Chen for Cu(II) removal using gum-arabic modified magnetic nanoadsorbent [33].

3.3. Effect of contact time

Equilibrium time is another important parameter to heavy metals wastewater treatment process. The

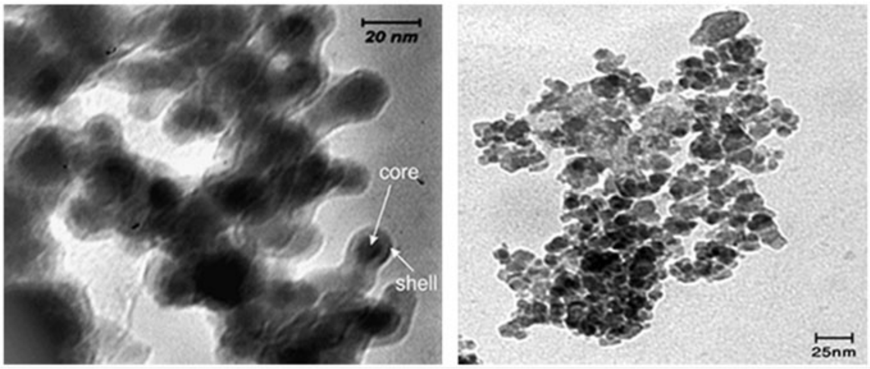

Fig. 2. TEM image of MALA.

effect of contact time on the removal of metal ions by 0.05 g MALA and 0.12 g ALA was studied separately over a time of 1–15 min with 100 mL of 100 mg L^{-1} metal ions solution (pH 6) at 25˚C. The removal percentages of metal ions by MALA and ALA as a function of contact time were illustrated in Fig. 4(a) and (b), respectively. Obviously, the adsorption rates of metal ions onto both the adsorbents were very rapid initially, which indicates that there are plenty of readily accessible sites. Then, the adsorption rates slowly decreased until it reached equilibrium in 10 and 7 min for MALA and ALA, respectively, and remained constant up to 15 min. This indicated that the adsorption of metal ions tended toward saturation at 10 and 7 min depending on the adsorbent type. This might be due to the fact that initially all adsorbent sites were vacant and the solute concentration gradient was high. However, after the initial period, slow adsorption may be due to slower diffusion of solute into the interior of the adsorbent [43]. Generally, the adsorption process of both the adsorbents for all the studied metal ions was fast when compared to previous studies [41,42,44–50]. Banerjee et al. attributed such a fast adsorption rate to the external surface adsorption [33]. Accordingly, the optimum contact times were selected as 7 and 10 min for all the subsequent studies involving ALA and MALA, respectively.

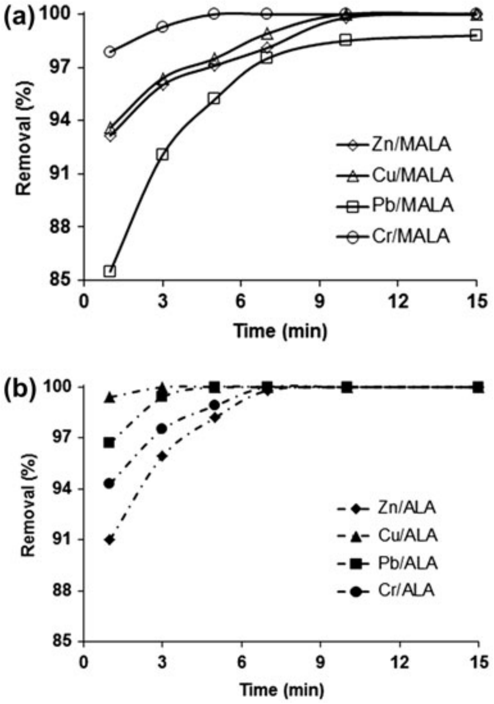

Fig. 4. Effect of contact time on the adsorption of metal ions onto (a) MALA, (100 mL of 100 mg L^{-1} metal ions solution; pH 6; mALA = 0.12 g, mMALA = 0.05 g; T = 25˚C), (b) ALA (100 mL of 100 mg L^{-1} metal ions solution; pH 6; mALA = 0.12 g, mMALA = 0.05 g; T = 25˚C).

3.4. Effect of amount and type of adsorbent

Adsorbent dosage is an important parameter because it determines the capacity of an adsorbent for a given initial concentration of the adsorbate [51]. Adsorption of metal ions was studied using different dosages of ALA and MALA (0.01–0.12 g) at the optimum pH and contact time. As shown in Fig. 5, percentage removal of metal ions enhances with the increase in adsorbent dosage. The maximum percent removal of all the studied metal ions was obtained with 0.05 g MALA and 0.1 g ALA; these were, therefore, selected for further experiments. Obviously, adsorption equilibrium was reached with low MALA dosage compared to the ALA, which can be attributed to its more available adsorption sites. However, for both the sorbents, higher dosages had no significant effect on the metal ions uptake as the surface metal ions concentration and the solution metal ions concentration came to equilibrium with each other. At low adsorbent dosages, the absorbent surface became saturated with the metal ions and the residual metal ions concentrations in the solution were large. As the adsorbent dosage increased, the adsorbent sites available for heavy metal ions are also increased and consequently better adsorption took place [52].

3.5. Effect of temperature

The adsorption experiments of metal ions were performed at six different temperatures in the range

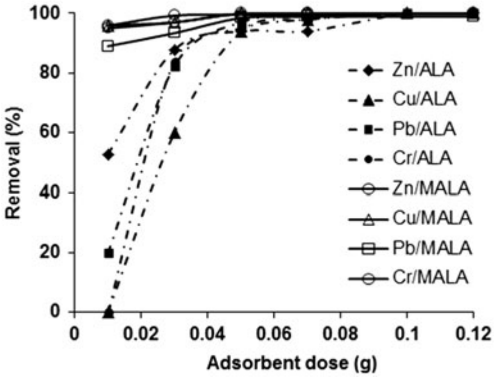

Fig. 5. Effect of adsorbent dosage on the adsorption of metal ions onto MALA and ALA (100 mL of 100 mg L^{-1} metal ions solution; pH 6; tALA = 7 min, tMALA = 10 min; T = 25˚C).

of 15–65 °C, with the conditions presented in Fig. 6. The removal percentage of metal ions decreased with the rise in solution temperature from 15 to 65 °C (Fig. 6). This is mainly due to the decreased surface activity suggesting that adsorption between metal ions and the sorbent was exothermic process. With increasing temperature, the attractive forces between the adsorbent surface and metal ions are weakened and then sorption decreases [53]. So, the adsorption of metal ions may involve mainly physical sorption. Similar results have also been reported on Zn(II) removal by both the bentonite and kaoline and Cu(II) removal by amino-modified magnetite nanoparticles [53,54].

3.6. Adsorption isotherms

Adsorption isotherms are used to describe adsorption equilibrium for wastewater treatments. In the present work, the sorption data have been subjected to different sorption isotherms, namely Langmuir, Freundlich, and Tempkin models. Langmuir adsorption isotherm is valid in the case of monolayer adsorption onto the surface with a finite number of identical sites [55]. Freundlich isotherm is used for the description of multilayer adsorption with interaction between adsorbed molecules [56]. The Tempkin isotherm model assumes that the adsorption energy decreases linearly with the surface coverage due to some indirect adsorbate/adsorbate interactions [57]. The linear forms of isotherm models are defined as:

$$\frac{C_e}{q_e} = \frac{1}{K_L q_{max}} + \frac{C_e}{q_{max}} \tag{7}$$

$$\ln q_e = \ln K_F + \frac{1}{n} \ln C_e \tag{8}$$

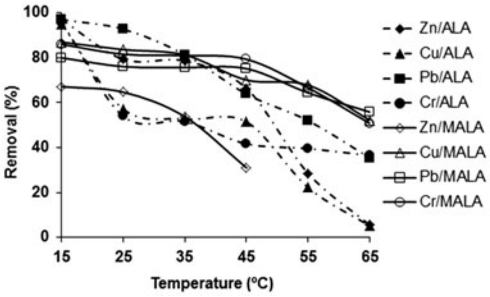

Fig. 6. Effect of temperature on the adsorption of metal ions onto MALA and ALA (pH 6; sample volume = 100 mL; for MALA: sorbate concentration 35 mg L^{-1}, $m = 0.005$ g, and $t = 10$ min; for ALA: sorbate concentration 65 mg L^{-1}, $m = 0.01$ g, $t = 7$ min).

$$q_e = B_T \ln K_T + B_T \ln C_e \tag{9}$$

The experimental equilibrium adsorption data were fitted to the above equations using plot of C_e/q_e vs. C_e, $\ln q_e$ vs. $\ln C_e$, and q_e vs. $\ln C_e$, respectively. Isotherm constants were determined from the slopes and intercepts of the corresponding linear plots. In Langmuir model, q_e is the amount of heavy metal ion adsorbed at equilibrium (mg g^{-1}), q_{max} is maximum adsorption capacity (mg g^{-1}) on unit mass of adsorbent, and K_L is the Langmuir constant (L mg^{-1}), related to the free energy of adsorption. Furthermore, the essential characteristic of the Langmuir isotherm, i.e. dimensionless separation factor (R_L) was calculated using Eq. (10). The R_L values between 0 and 1 indicate favorable adsorption [58]. In Freundlich isotherm, K_F ($mg^{1-(1/n)}$ $L^{1/n}$ g^{-1}) and n are the isotherm constants related to adsorption capacity and adsorption intensity, respectively. If $1 < n < 10$, the adsorption is favorable. In Tempkin model, K_T is the equilibrium binding constant (L mg^{-1}) and B_T is a constant related to adsorption heat (kJ mol^{-1}).

$$R_L = \frac{1}{1 + K_L C_0} \tag{10}$$

The results obtained by fitting the experimental equilibrium adsorption data to the isotherm models together with the correlation coefficients (R^2) for all the models were presented in Table 1. Examination of the linear isotherm plots suggested that, for the adsorption of metal ions onto MALA and ALA adsorbents, the Langmuir isotherm yielded a much better fit with higher correlation coefficient ($R^2 > 99\%$) than the other models. Also, the values of R_L are in the range of 0–1, which confirms the favorable uptake of metal ions by both the adsorbents. Therefore, uptake of Pb(II), Cu(II), Zn(II), and Cr(III) ions by MALA and ALA preferably followed the monolayer adsorption process. This is in agreement with the results obtained by Li et al. for the adsorption of Cu(II), Pb(II), Cr(III) ions by sawdust and modified peanut husk [59].

A comparison of the maximum adsorption capacities of different adsorbents for Pb(II), Cu(II), Zn(II), and Cr(III) ions was also reported in Table 2. The variation in maximum adsorption capacities between the adsorbents could be related to the type and concentration of surface groups responsible for adsorption of metal ions from the solution. Obviously, the adsorption capacity of MALA used in the present study is significant. In addition, MALA was more effective in the removal of Cu(II) and Cr(III) ions than ALA. The amount of same ions adsorbed per gram of

Table 1
Isotherm parameters for metal ions removal by ALA and MALA (sorbate concentration 25–100 mg L^{-1}; $m_{MALA} = 0.005$ g, $m_{ALA} = 0.01$ g)

Meal ion	Langmuir				Freundlich			Temkin		
	q_{max} (mg/g)	K_L (L/mg)	R_L[a]	R^2	K_F	n	R^2	K_T (L/mg)	B_T (kJ/mol)	R^2
MALA										
Pb(II)	333.3	0.13	0.071	0.996	83.67	2.86	0.755	1.21	86.53	0.756
Cu(II)	345.0	0.25	0.038	0.991	155.24	3.3	0.778	1.60	114.00	0.791
Cr(III)	333.3	0.28	0.034	0.997	135.55	3.37	0.821	1.45	99.97	0.877
Zn(II)	71.4	0.48	0.020	0.983	23.95	3.37	0.851	1.38	21.56	0.856
ALA										
Pb(II)	500.0	0.89	0.011	0.998	275.61	5.92	0.813	47.84	67.00	0.805
Cu(II)	117.6	0.52	0.019	0.995	433.93	3.14	0.985	345.08	65.68	0.975
Cr(III)	142.8	0.71	0.014	0.986	349.35	3.47	0.625	394.31	57.36	0.896
Zn(II)	200.0	0.81	0.012	0.998	376.98	6.03	0.885	5,770.27	41.31	0.887

[a] For $C_0 = 100$ mg L^{-1}.

Table 2
Comparison of maximum adsorption capacities of different magnetic and non-magnetic low-cost adsorbents for removal of metal ions

Adsorbent	q_{max} (mg g^{-1})				Ref.
	Pb^{2+}	Cu^{2+}	Zn^{2+}	Cr^{3+}	
Cocoa shells	–	2.87	2.92	2.52	[46]
Pleurotus ostreatus	–	8.06	3.22	10.75	[65]
Modified sugarcane bagasse	196	114	–	–	[66]
Modified carrot residues	–	32.74	29.61	45.09	[67]
Olive leaves ash	90.91	62.50	–	142.85	[23]
Rice husk ash	12.00	4.03	–	–	[68]
Date palm leaf ash	31.84	–	–	–	[69]
Ficus religiosa leaves ash	68.03	–	–	–	[70]
Zeolite	–	88	111	45	[50]
Maghemite nanotubes	71.42	111.1	84.95	–	[71]
Fe_3O_4 nanoadsorbents	36	–	–	–	[49]
Magnetic zeolite	–	87	114	49	[50]
Fe_3O_4 NPs[a]-immobilized sand	2.08	1.26	–	–	[72]
Pectin-coated iron oxide nanocomposite	–	48.99	–	–	[45]
Gum arabic-modified magnetic NPs[a]	–	38.50	–	–	[33]
Magnetic chitosan NPs[a]	–	35.50	–	–	[48]
ALA	500.0	117.6	200.0	142.8	This study
MALA	333.3	345.0	333.3	71.4	This study

[a] Nanoparticles.

MALA was more than twice that of ALA, revealing the modification of ALA indeed could enhance the adsorption capability. Therefore, MALA is considered to be a potential low-cost nanoadsorbent for heavy metal ions removal from aqueous solutions.

3.7. Adsorption kinetics

Adsorption kinetics has been proposed to elucidate the adsorption mechanism. The mechanism of adsorption depends on the physical and chemical characteristics of the adsorbent as well as on the mass transport process. In order to investigate the mechanism of metal ions adsorption on the adsorbents and examine the potential rate-controlling step, i.e. mass transfer or chemical reaction, different kinetic models were studied. The capability of Lagergren's pseudo-first-order, pseudo-second-order, and intraparticle diffusion models was examined in this study. The correlation coefficient (R^2, close or equal to 1) was introduced to evaluate the suitability of different models. The linearized-integral forms of studied kinetic models are expressed as [60–62]:

$$\ln\left(q_1 - q_t\right) = \ln q_1 - k_1 t \tag{11}$$

$$\frac{t}{q_t} = \frac{1}{k_2 q_2^2} + \frac{t}{q_2} \tag{12}$$

$$q_t = k_\mathrm{i}\, t^{1/2} + C_\mathrm{i} \tag{13}$$

In pseudo-first-order and pseudo-second-order kinetic models, q_1 (or q_2) and q_t (mg g^{-1}) are the values of amount adsorbed per unit mass of sorbent at equilibrium and at any time, k_1 (min^{-1}) is the pseudo-first-order adsorption rate coefficient and k_2 (g mg^{-1} min^{-1}) is the pseudo-second-order constant. In intraparticle diffusion model, k_i (mg g^{-1} min$^{-1/2}$) is the diffusion rate coefficient and C_i is the intercept and relates to the thickness of the boundary layer. The parameter values for each model were obtained from the respective linear plots of ln (q_1–q_2) vs. t, t/q_t vs. t, and q_t vs. $t^{1/2}$, respectively.

The results along with R^2 values were listed in Table 3. Comparing the correlation coefficients of kinetic models revealed that for both the adsorbents, the pseudo-second-order kinetic model with R^2 values close to 1 matched better the experimental data than the other models. This model is based on the assumption that the rate-limiting step may be a chemical sorption involving valence forces through sharing or exchange of electrons between the adsorbent and the adsorbate [63]. Similar results have also been reported for heavy metal ions removal by the other adsorbents. [45,54,59].

3.8. Adsorption thermodynamics

Thermodynamic studies are used to decipher any reaction in a better way. In the present study, the variation in the extent of adsorption with respect to temperature has been explained based on thermodynamic parameters viz. changes in standard free energy (ΔG°), enthalpy (ΔH°), and entropy (ΔS°). Thermodynamic parameters were evaluated in the temperatures range of 21–37°C. The values of the thermodynamic parameters were calculated using the thermodynamic equations described below [52]:

$$\Delta G^\circ = -RT \ln K_\mathrm{c} \tag{14}$$

$$\ln K_\mathrm{c} = \frac{\Delta S^\circ}{R} - \frac{\Delta H^\circ}{RT} \tag{15}$$

where R is the ideal gas constant (8.314 J mol^{-1} K^{-1}), T is the absolute temperature (K), and K_c is the thermodynamic equilibrium constant defined by $q_\mathrm{e}/C_\mathrm{e}$. ΔH° and ΔS° values were obtained from slope and intercept of the plot ln K_c vs. $1/T$.

The values of the thermodynamic parameters for both the adsorbents were presented in Table 4. Negative ΔH° values at different temperatures suggested the exothermic nature of the adsorption process, which was in good agreement with the results that the adsorption of metal ions decreases with the increasing temperature. Negative ΔG° values indicated that the sorption of metal ions was feasible and spontaneous under the conditions applied. The negative values of entropy indicated the decreased randomness at the solid/solution interface, while positive values of entropy showed an increased randomness during metal ions adsorption. Study carried out by Panadare et al. on Cu (II) removal by waste sweet lime peel, showed similar results [63].

3.9. Comparison of heavy metal ions removal in single and mixed systems

The adsorption capacities of heavy metal ions by both the adsorbents in the single and mixed metal ions systems were examined and the results were depicted in Fig. 7. Obviously, under the optimized conditions, the adsorption capacities of both MALA and ALA for mixed metal ions system were lower than those obtained for the single system. This is due to the competitive adsorption of metal ions in the mixed system and their antagonistic effect, which decreases the uptake of all the metal ions form the solution. Furthermore, in the single metal ion system, MALA has higher sorption capacities for all the metal ions compared to ALA. The adsorption capacities of the adsorbents for mixed system decreased in the order of $\mathrm{Cu^{2+} > Pb^{2+}}$, $\mathrm{Cr^{3+} > Zn^{2+}}$ for MALA, and $\mathrm{Pb^{2+} > Zn^{2+} > Cr^{3+} > Cu^{2+}}$ for ALA. This is probably due to a different electrostatic attraction between heavy metal cations and negatively charged

Table 3
Kinetic parameters for metal ions removal by ALA and MALA (sorbate concentration 100 mg L^{-1}; t = 1–20 min; m_{MALA} = 0.005 g, m_{ALA} = 0.01 g)

Metal ions	Pseudo-first-order kinetic			Pseudo-second-order kinetic			Intra-particle diffusion		
	q_1 (mg/g)	K_1	R^2	q_2 (mg/g)	K_2	R^2	K_i	C_i	R^2
MALA									
Pb(II)	27.98	0.11	0.97	204	0.02	0.99	8.55	162.5	0.81
Cu(II)	12.30	0.12	0.77	208.3	0.02	0.99	3.34	185.5	0.94
Cr(III)	3.58	0.14	0.90	204	0.04	0.99	1.07	195.6	0.78
Zn(II)	15.52	0.17	0.98	200	0.03	0.99	2.98	186.4	0.58
ALA									
Pb(II)	205	0.08	0.92	227.27	1.2	0.98	29.6	67.1	0.95
Cu(II)	270	0.11	0.77	303.03	2.1	0.99	44.6	64.6	0.93
Cr(III)	180	0.10	0.84	238.09	4.2	0.99	38.9	1.7	0.95
Zn(II)	270	0.15	0.88	333.33	1.3	0.99	49.4	43.3	0.91

Table 4
Thermodynamic parameters of metal ions removal at 25℃ (for MALA: sorbate concentration 35 mg L^{-1}; t = 10 min; m_{MALA} = 0.005 g for ALA: sorbate concentration 65 mg L^{-1}; t = 7 min; m_{ALA} = 0.01 g)

Metal ions	ΔG° (kJ/mol)	ΔH° (kJ/mol)	ΔS° (kJ/mol K)
MALA			
Pb(II)	−10,856.80	−5,904.00	16.62
Cu(II)	−11,919.70	−2,167.20	32.73
Cr(III)	−10,415.80	−6,690.50	12.50
Zn(II)	−11,179.00	−11,848.30	−2.24
ALA			
Pb(II)	−8,426.71	63,219.66	240.42
Cu(II)	−9,139.46	−30,454.00	−71.53
Cr(III)	−7,804.06	−31,861.70	−80.73
Zn(II)	−8,840.60	−42,938.50	−114.42

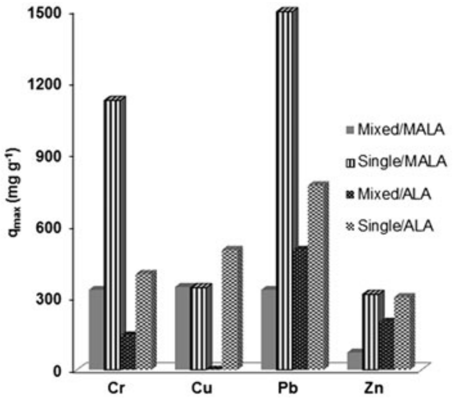

Fig. 7. Comparison of $q_{\max}$ values of metal ions in the single and mixed solutions.

adsorption sites, mainly related to the hydrated ionic radii of the studied heavy metals. Study carried out by Liu et al. using steel slag adsorbent showed similar results, in which the adsorption of Pb(II), Cu(II), Zn(II), and Cr(III) ions decreased in the mixed system compared to the single system [64].

3.10. Desorption and reusability of MALA

The economic possibility of adsorbent is one of the major concerns among its applications. It is widely estimated by the reusability of adsorbent. To test the possibility of regeneration and reusability of MALA, the spent adsorbents were washed with 0.001 M HCl solution of pH values between 2 and 3 until no detectable heavy metal ions were observed in the washing solution, as confirmed by the FAAS. After that, MALA sorbents were thoroughly washed with deionized water till the pH of the water reached the range of 5.0–6.5. Then, the regenerated adsorbents were vacuum-dried and reused for the subsequent adsorption cycle. Five cycles of consecutive adsorption–desorption–regeneration were carried out to validate the reusability of MALA for the removal of heavy metal ions from aqueous solutions. As shown in Table 5, the removal percentages of metal ions decreased gradually with increasing regeneration cycle number. The value of cycle 0 was denoted as the adsorption of the original MALA. After the first regeneration cycle, the removal efficiencies were 94.49, 95.14, 97.83, and 93.89% for Pb(II), Cu(II), Cr(III), and Zn(II) ions, respectively. After the fifth cycle, the removal percentages of Pb(II), Cu(II), Cr(III), and

Table 5
Reusability study of MALA

Cycle number	$n = 0$	$n = 1$	$n = 2$	$n = 3$	$n = 4$	$n = 5$
Metal ion	Removal (%)					
Pb(II)	98.50	94.49	89.35	84.73	78.85	71.64
Cu(II)	100	95.14	94.60	92.87	90.12	88.15
Cr(III)	100	97.83	96.87	94.95	93.14	92.08
Zn(II)	99.42	93.89	92.54	90.72	88.56	86.67

Zn(II) ions were 71.64, 88.15, 92.08, and 86.67%, respectively, indicating that MALA adsorbent had the potential for reusability. The results demonstrated that the MALA can be employed as an excellent reusable nanoadsorbent for the removal of the metal ions from aqueous solutions.

4. Conclusions

The potential of the magnetically modified ALA as a novel low-cost nanoadsorbent for simultaneous removal of Pb(II), Cu(II), Zn(II), and Cr(III) ions from aqueous solutions were investigated. The batch adsorption parameters for both the magnetic and non-magnetic ALA were studied and optimized. In optimum conditions for removal of proposed metal ions (100 mL, 100 mg L^{-1}), contact time and adsorbent amount were obtained 7 min and 0.1 g with ALA and 10 min and 0.05 g with MALA at pH 6 and 25°C. The equilibrium adsorption data were well fitted by the Langmuir isotherm model. The adsorption process was fast and pseudo-second-order rate model accurately described the kinetics of the adsorption, which suggested chemisorption as the rate-limiting step in the adsorption process. The results suggested that MALA was highly efficient for simultaneous adsorption of heavy metal ions from aqueous solutions with maximum capacities of 333, 345, 71.4, and 333 mg g^{-1} for Pb(II), Cu(II), Zn(II), and Cr(III) ions, respectively. Based on thermodynamic studies, the adsorption process of all the metal ions was both exothermic and spontaneous. Desorption studies revealed the reusability of MALA after its treatment with HCl solution. According to results, MALA can be well recommended for wastewater treatments and control of environmental pollution.

Acknowledgments

The authors wish to thank Semnan University Scientific Research Foundation for financial support.

References

[1] F. Boudrahem, A. Soualah, F. Aissani-Benissad, Pb(II) and Cd (II) removal from aqueous solutions using activated carbon developed from coffee residue activated with phosphoric acid and zinc chloride, J. Chem. Eng. Data 56 (2011) 1946–1955.

[2] F. Mohammed-Azizi, S. Dib, M. Boufatit, Removal of heavy metals from aqueous solutions by Algerian bentonite, Desalin. Water Treat. 51 (2013) 4447–4458.

[3] F. Fu, Q. Wang, Removal of heavy metal ions from wastewaters: A review, J. Environ. Manage. 92 (2011) 407–418.

[4] C. Fersi Bennani, O. M'hiri, Comparative study of the removal of heavy metals by two nanofiltration membranes, Desalin. Water Treat. 53 (2015) 1024–1030.

[5] J. Yoon, G. Amy, J. Chung, J. Sohn, Y. Yoon, Removal of toxic ions (chromate, arsenate, and perchlorate) using reverse osmosis, nanofiltration, and ultrafiltration membranes, Chemosphere 77 (2009) 228–235.

[6] M. Naushad, A. Mittal, M. Rathore, V. Gupta, Ion-exchange kinetic studies for Cd(II), Co(II), Cu(II), and Pb (II) metal ions over a composite cation exchanger, Desalin. Water Treat. 54 (2015) 2883–2890.

[7] H. Polat, D. Erdogan, Heavy metal removal from waste waters by ion flotation, J. Hazard. Mater. 148 (2007) 267–273.

[8] S. Ahluwalia, D. Goyal, Removal of heavy metals by waste tea leaves from aqueous solution, Eng. Life Sci. 5 (2005) 158–162.

[9] T. Bohli, A. Ouederni, N. Fiol, I. Villaescusa, Single and binary adsorption of some heavy metal ions from aqueous solutions by activated carbon derived from olive stones, Desalin. Water Treat. 53 (2015) 1082–1088.

[10] M. Ahmaruzzaman, Industrial wastes as low-cost potential adsorbents for the treatment of wastewater laden with heavy metals, Adv. Colloid Interface Sci. 166 (2011) 36–59.

[11] T.A. Kurniawan, G. Chan, W.-H. Lo, S. Babel, Comparisons of low-cost adsorbents for treating wastewaters laden with heavy metals, Sci. Total Environ. 366 (2006) 409–426.

[12] D. Sud, G. Mahajan, M. Kaur, Agricultural waste material as potential adsorbent for sequestering heavy metal ions from aqueous solutions–A review, Bioresour. Technol. 99 (2008) 6017–6027.

[13] T. Zewail, S. El-Garf, Preparation of agriculture residue based adsorbents for heavy metal removal, Desalin. Water Treat. 22 (2010) 363–370.

[14] W. Wan Ngah, M. Hanafiah, Removal of heavy metal ions from wastewater by chemically modified plant wastes as adsorbents: A review, Bioresour. Technol. 99 (2008) 3935–3948.

[15] C.G. Rocha, D.A.M. Zaia, R.V.d.S. Alfaya, A.A.d.S. Alfaya, Use of rice straw as biosorbent for removal of Cu(II), Zn(II), Cd(II) and Hg(II) ions in industrial effluents, J. Hazard. Mater. 166 (2009) 383–388.

[16] N. Miralles, C. Valderrama, I. Casas, M.a. Martínez, A. Florido, Cadmium and lead removal from aqueous solution by grape stalk wastes: Modeling of a fixed-bed column, J. Chem. Eng. Data. 55 (2010) 3548–3554.

[17] J. Igwe, A. Abia, Adsorption kinetics and intraparticulate diffusivities for bioremediation of Co(II), Fe(II) and Cu(II) ions from waste water using modified and unmodified maize cob, Int. J. Phys. Sci. 2 (2007) 119–127.

[18] A. Ghosh, K. Sinha, P.D. Saha, Central composite design optimization and artificial neural network modeling of copper removal by chemically modified orange peel, Desalin. Water Treat. 51 (2013) 7791–7799.

[19] H. Jaman, D. Chakraborty, P. Saha, A study of the thermodynamics and kinetics of copper adsorption using chemically modified rice husk, Clean—Soil Air Water 37 (2009) 704–711.

[20] V. Sarin, K.K. Pant, Removal of chromium from industrial waste by using eucalyptus bark, Bioresour. Technol. 97 (2006) 15–20.

[21] A. Al Bsoul, The use of eucalyptus leaves as adsorbent for copper ion removal, Desalin. Water Treat. 52 (2014) 7838–7844.

[22] L. Hu, A.A. Adeyiga, T. Greer, E. Miamee, A. Adeyiga, Removal of metal ions from wastewater with roadside tree leaves, Chem. Eng. Commun. 189 (2002) 1587–1597.

[23] H. Zavvar Mousavi, Z. Lotfi, Adsorption of heavy metal ions on olive leaves: Equilibrium and kinetic studies, J. Appl. Chem. 7 (2012) 49–56.

[24] L. Bouziane, F. Bendebane, F. Ismail, R. Delimi, Removal of zinc and cadmium from an aqueous solution using sawdust as a low-cost adsorbent: Application of Plackett-Burman design, Desalin. Water Treat. 49 (2012) 189–199.

[25] Y. Bulut, Z. Tez, Removal of heavy metals from aqueous solution by sawdust adsorption, J. Environ. Sci. 19 (2007) 160–166.

[26] D. Mohan, A. Sarswat, V.K. Singh, M. Alexandre-Franco, C.U. Pittman Jr, Development of magnetic activated carbon from almond shells for trinitrophenol removal from water, Chem. Eng. J. 172 (2011) 1111–1125.

[27] A.-F. Ngomsik, A. Bee, M. Draye, G. Cote, V. Cabuil, Magnetic nano-and microparticles for metal removal and environmental applications: A review, C.R. Chim. 8 (2005) 963–970.

[28] T. Indira, P. Lakshmi, Magnetic nanoparticles—A review, Int. J. Pharm. Sci. Nanotechnol. 3 (2010) 1035–1042.

[29] I. Safarik, K. Horska, B. Svobodova, M. Safarikova, Magnetically modified spent coffee grounds for dyes removal, Eur. Food Res. Technol. 234 (2012) 345–350.

[30] D. Zhang, S. Wei, C. Kaila, X. Su, J. Wu, A.B. Karki, D.P. Young, Z. Guo, Carbon-stabilized iron nanoparticles for environmental remediation, Nanoscale 2 (2010) 917–919.

[31] P. Panneerselvam, N. Morad, K.A. Tan, Magnetic nanoparticle (Fe_3O_4) impregnated onto tea waste for the removal of nickel(II) from aqueous solution, J. Hazard. Mater. 186 (2011) 160–168.

[32] S.Y. Yeo, S. Choi, V. Dien, Y.K. Sow-Peh, G. Qi, T.A. Hatton, P.S. Doyle, B.J.R. Thio, Using magnetically responsive tea waste to remove lead in waters under environmentally relevant conditions, PLoS One 8 (2013) e66648.

[33] S.S. Banerjee, D.-H. Chen, Fast removal of copper ions by gum arabic modified magnetic nano-adsorbent, J. Hazard. Mater. 147 (2007) 792–799.

[34] I. Safarik, K. Horska, M. Safarikova, Magnetically modified spent grain for dye removal, J. Cereal Sci. 53 (2011) 78–80.

[35] I. Safarik, M. Safarikova, Magnetic fluid modified peanut husks as an adsorbent for organic dyes removal, Phys. Proc. 9 (2010) 274–278.

[36] K.A. Tan, N. Morad, T.T. Teng, I. Norli, P. Panneerselvam, Removal of cationic dye by magnetic nanoparticle (Fe_3O_4) impregnated onto activated maize cob powder and kinetic study of dye waste adsorption, APCBEE Proc. 1 (2012) 83–89.

[37] K. Eshun, Q. He, Aloe vera: A valuable ingredient for the food, pharmaceutical and cosmetic industries—A review, Crit. Rev. Food Sci. Nutr. 44 (2004) 91–96.

[38] C. Pragathiswaran, S. Sibi, P. Sivanesan, Adsorption of hexavalent chromium from aqueous solutions by aloe vera leaf, Int. J. Res. Pharm. Chem. 3 (2013) 876–880.

[39] S. Laurent, D. Forge, M. Port, A. Roch, C. Robic, L. Vander Elst, R.N. Muller, Magnetic iron oxide nanoparticles: Synthesis, stabilization, vectorization, physicochemical characterizations, and biological applications, Chem. Rev. 108 (2008) 2064–2110.

[40] M. Saifuddin, P. Kumaran, Removal of heavy metal from industrial wastewater using chitosan coated oil palm shell charcoal, Electron. J. Biotechnol. 8 (2005) 43–53.

[41] O.E. Abdel Salam, N.A. Reiad, M.M. ElShafei, A study of the removal characteristics of heavy metals from wastewater by low-cost adsorbents, J. Adv. Res. 2 (2011) 297–303.

[42] O. Moradi, B. Mirza, M. Norouzi, A. Fakhri, Removal of Co(II), Cu(II) and Pb(II) ions by polymer based 2-hydroxyethyl methacrylate: thermodynamics and desorption studies, Iran. J. Environ. Health Sci. Eng. 9 (2012) 31–33.

[43] B. Amarasinghe, R. Williams, Tea waste as a low cost adsorbent for the removal of Cu and Pb from wastewater, Chem. Eng. J. 132 (2007) 299–309.

[44] A. Bhattacharya, S. Mandal, S. Das, Adsorption of Zn(II) from aqueous solution by using different adsorbents, Chem. Eng. J. 123 (2006) 43–51.

[45] J.-L. Gong, X.-Y. Wang, G.-M. Zeng, L. Chen, J.-H. Deng, X.-R. Zhang, Q.-Y. Niu, Copper(II) removal by pectin–iron oxide magnetic nanocomposite adsorbent, Chem. Eng. J. 185–186 (2012) 100–107.

[46] N. Meunier, J. Laroulandie, J. Blais, R. Tyagi, Cocoa shells for heavy metal removal from acidic solutions, Bioresour. Technol. 90 (2003) 255–263.

[47] Y.-T. Zhou, H.-L. Nie, C. Branford-White, Z.-Y. He, L.-M. Zhu, Removal of Cu^{2+} from aqueous solution by chitosan-coated magnetic nanoparticles modified with α-ketoglutaric acid, J. Colloid Interface Sci. 330 (2009) 29–37.

[48] C. Yuwei, W. Jianlong, Preparation and characterization of magnetic chitosan nanoparticles and its application for Cu(II) removal, Chem. Eng. J. 168 (2011) 286–292.

[49] N.N. Nassar, Rapid removal and recovery of Pb(II) from wastewater by magnetic nanoadsorbents, J. Hazard. Mater. 184 (2010) 538–546.

[50] L.C. Oliveira, D.I. Petkowicz, A. Smaniotto, S.B. Pergher, Magnetic zeolites: A new adsorbent for removal of metallic contaminants from water, Water Res. 38 (2004) 3699–3704.

[51] Y. Bulut, Z. Baysal, Removal of Pb(II) from wastewater using wheat bran, J. Environ. Manage. 78 (2006) 107–113.

[52] T.K. Naiya, A.K. Bhattacharya, S.K. Das, Adsorption of Cd(II) and Pb(II) from aqueous solutions on activated alumina, J. Colloid Interface Sci. 333 (2009) 14–26.

[53] T.K. Sen, C. Khoo, Adsorption characteristics of zinc (Zn^{2+}) from aqueous solution by natural bentonite and kaolin clay minerals: A comparative study, Comput. Water Energy Environ. Eng. 2 (2013) 1–6.

[54] Y. Lin, H. Chen, K. Lin, B. Chen, C. Chiou, Application of magnetic particles modified with amino groups to adsorb copper ions in aqueous solution, J. Environ. Sci. 23 (2011) 44–50.

[55] I. Langmuir, The adsorption of gases on plane surfaces of glass, mica and platinum, J. Am. Chem. Soc. 40 (1918) 1361–1403.

[56] H. Freundlich, Adsorption in solutions, Phys. Chem. Soc. 40 (1906) 1361–1368.

[57] M. Temkin, V. Pyzhev, Recent modifications to Langmuir isotherms, Acta Physiochim. USSR 12 (1940) 217–222.

[58] K. Hall, L. Eagleton, A. Acrivos, T. Vermeulen, Pore- and solid-diffusion kinetics in fixed-bed adsorption under constant-pattern conditions, Ind. Eng. Chem. Fund. 5 (1966) 212–223.

[59] Q. Li, J. Zhai, W. Zhang, M. Wang, J. Zhou, Kinetic studies of adsorption of Pb(II), Cr(III) and Cu(II) from aqueous solution by sawdust and modified peanut husk, J. Hazard. Mater. 141 (2007) 163–167.

[60] Y.-S. Ho, G. McKay, Pseudo-second order model for sorption processes, Process Biochem. 34 (1999) 451–465.

[61] S. Lagergren, About the theory of so-called adsorption of soluble substances, Kung. Sven. Veten. Hand. 24 (1898) 1–39.

[62] W. Weber, J. Morris, Kinetics of adsorption on carbon from solution, J. Sanit. Eng. Div. Am. Soc. Civ. Eng 89 (1963) 31–60.

[63] D.C. Panadare, V.G. Lade, V.K. Rathod, Adsorptive removal of copper(II) from aqueous solution onto the waste sweet lime peels (SLP): Equilibrium, kinetics and thermodynamics studies, Desalin. Water Treat. 52 (2014) 7822–7837.

[64] S. Liu, J. Gao, B. Qu, Y. Yang, X. Xin, Using steel slag adsorbent showed similar results, in which the adsorption of Pb(II), Cu(II), Zn(II), and Cr(III) ions decreased in the mixed system compared to the single system, 11th International Conference on Enviromental Science and Technology, Chania-Crete, Greece, 2009, p. A740–A747.

[65] A. Javaid, R. Bajwa, U. Shafique, J. Anwar, Removal of heavy metals by adsorption on *Pleurotus ostreatus*, Biomass Bioenergy 35 (2011) 1675–1682.

[66] O. Karnitz Jr, L.V.A. Gurgel, J.C.P. de Melo, V.R. Botaro, T.M.S. Melo, R.P. de Freitas Gil, L.F. Gil, Adsorption of heavy metal ion from aqueous single metal solution by chemically modified sugarcane bagasse, Bioresour. Technol. 98 (2007) 1291–1297.

[67] B. Nasernejad, T.E. Zadeh, B.B. Pour, M.E. Bygi, A. Zamani, Camparison for biosorption modeling of heavy metals (Cr(III), Cu(II), Zn(II)) adsorption from wastewater by carrot residues, Process Biochem. 40 (2005) 1319–1322.

[68] M. Vieira, A. Almeida Neto, M. Silva, C. Carneiro, A. Melo Filho, Adsorption of lead and copper ions from aqueous effluents on rice husk ash in a dynamic system, Braz. J. Chem. Eng. 31 (2014) 519–529.

[69] F. Ghorbani, A. Sanati, H. Younesi, A. Ghoreyshi, The potential of date-palm leaf ash as low-cost adsorbent for the removal of Pb(II) ion from aqueous solution, Int. J. Eng. Trans. B. 25 (2012) 269–278.

[70] S. Qaiser, A.R. Saleemi, M. Umar, Biosorption of lead from aqueous solution by *Ficus religiosa* leaves: Batch and column study, J. Hazard. Mater. 166 (2009) 998–1005.

[71] A. Roy, J. Bhattacharya, Removal of Cu(II), Zn(II) and Pb(II) from water using microwave-assisted synthesized maghemite nanotubes, Chem. Eng. J. 211–212 (2012) 493–500.

[72] S.-M. Lee, C. Laldawngliana, D. Tiwari, Iron oxide nano-particles-immobilized-sand material in the treatment of Cu(II), Cd(II) and Pb(II) contaminated waste waters, Chem. Eng. J. 195–196 (2012) 103–111.